Journal of Hydrology (2006) **328**, 83–97

available at www.sciencedirect.com

SCIENCE DIRECT®

journal homepage: www.elsevier.com/locate/jhydrol

# Radar calibration by gage, disdrometer, and polarimetry: Theoretical limit caused by the variability of drop size distribution and application to fast scanning operational radar data

**GyuWon Lee *, Isztar Zawadzki**

*J.S. Marshall Radar Observatory, McGill University, P.O. Box 198, Macdonald Campus, Ste-Anne de Bellevue, Canada QC H9X 3V9*

Received 8 October 2002; received in revised form 16 April 2004; accepted 30 November 2005

**KEYWORDS**
Variability of drop size distribution;
Radar calibration;
Gage;
Disdrometer;
Polarimetry;
Drop deformation

**Summary** A long time record of drop size distributions (DSDs) is used to evaluate the effect of the DSD variability on the accuracy of radar adjustment by comparison with a rain gage on a daily basis. Radar and gage measurements are simulated from DSDs. When a single $R$—$Z$ relationship is used in the adjustment of the radar as a hydrological instrument, a standard deviation of fractional error of ~28% is expected. This uncertainty is related to the DSD variability in time. A calibration of reflectivity can be done if a disdrometer is available. This disdrometric radar calibration is not affected by the DSD variability. Thus, the uncertainty that is expected in the radar adjustment with a gage is eliminated. Some uncertainty in radar-disdrometer comparison due to the difference in sampling volumes is minimized by applying a sequential intensity filtering technique (SIFT). Good correlations between radar and disdrometric reflectivities indicate that this could be an excellent way of calibrating radar on a daily basis when a disdrometer is located at close range (less than 30 km) from radar. Furthermore, the consistency of independent checks of radar calibration error with different disdrometers and polarimetry validates the argument that the radar-disdrometer comparison can be used as a tool for absolute radar calibration.

The information from the McGill operational S-band polarimetric radar is also used to calibrate radar. This method is based on the fact that the specific differential phase shift ($K_{DP}$) or differential phase shift ($\Phi_{DP}$) between the horizontal and vertical polarized beams is immune to the radar calibration error whereas the reflectivity is affected by the calibration error. Due to the

* Corresponding author. Tel.: +1 514 398 7733; fax: +1 514 398 7755.
*E-mail address:* gwlee@zephyr.meteo.mcgill.ca (G. Lee).

0022-1694/$ - see front matter 
doi:10.1016/j.jhydrol.2005.11.046

variability of DSDs only, the uncertainty in polarimetric calibration is the standard deviation of 1 dB with a single parameter $K_{DP}$ and reduces to 0.5 dB when the differential reflectivity ($Z_{DR}$) is added as well. To guarantee the stability of this calibration method, data longer than at least an hour is necessary to calculate the calibration error for the fast scanning McGill operational polarimetric radar and contamination by bright band or snow should be avoided. The sensitivity of this calibration method with respect to the drop deformation is tested.


## Introduction

When considering radar calibration there are several areas of interest. On the one hand, the stability of the electronic equipment is a concern in its own right. On the other hand, possible effects of radome on the measurements are a problem that could depend on the state of the radome, whether dry, wet, or with rain streaks. In hydrological applications, calibration of the radar may imply some adjustment to ground truth. That is, the mean bias derived from radar-ground truth comparison can be applied to modify radar measurement. However, the differences between the radar measurements and precipitation intensity at ground may be caused by the height of the radar measurement coupled with the vertical profile of reflectivity, contamination by non-meteorological target, different sampling volume, etc. (Wilson and Brandes, 1979; Zawadzki, 1984; Joss and Lee, 1995; Smyth and Illingworth, 1998; Germann, 2000; Zawadzki et al., 2002; Lee, 2003). When a gage is used as the ground truth, the transformation of radar reflectivity into rain rate is another source of discrepancy (Joss and Waldvogel, 1970; Richard and Crozier, 1983; Doelling et al., 1998; Lee and Zawadzki, 2005a,b). As a result, the mean bias can change event by event even though the radar hardware is stable. Therefore, the mean bias cannot be referred to as a radar calibration error since it is not solely related to the stability of radar. Thus, the use of ground truth such as gage to correct radar measurement is often known as a ''radar adjustment'' and the mean bias is referred to as an ''adjustment bias.'' When these sources of errors are eliminated, the mean bias is related to the absolute stability of radar and can be referred to as a ''radar calibration'' error. Thus, the elimination of these sources of errors is required to use ground truth for the ''radar calibration.''

When a disdrometer is used for the comparison, the transformation with $R$—$Z$ relationships is not necessary because reflectivity can be determined from the drop-size distribution (DSD). However, the sources of errors listed earlier should still be minimized. Differences due to the sampling volume can be reduced by a using long term dataset. Precipitation growth or decay between heights of radar measurement and the ground can be significant for short period due to strong evaporation or interaction of drops. However, in our latitudes there is no significant change of reflectivity (less than 1 dB) below the bright band when a relatively long time is considered (see Fig. 10 in Fabry and Zawadzki, 1995). Therefore, when the radar hardware is relatively stable, the disdrometer data of at least a day can be used for ''radar calibration'' with tolerable uncertainty and the mean bias will be considered as the ''radar calibration error.''

Instead of adjusting radar information to ground truth, radar calibration with radar data themselves is a main priority and provides an independent monitoring of the performance of system. In this sense, additional information from polarimetric radar is a good candidate for the self-consistent radar calibration. Due to inherent characteristics, the specific differential phase shift $K_{DP}$ or differential phase shift $\Phi_{DP}$ between horizontal and vertical polarized beams is immune to the radar calibration (Zrnic and Ryzhkov, 1999). Hence, the combination of $Z_h$ and phase information is one way of monitoring the radar calibration. However, the phase information is noisy (Doviak and Zrnic, 1993) and pixel information can hardly be used in a fast scanning operational radar. In addition, the polarimetric calibration requires sufficiently heavy rain and/or a large spatial extent of precipitation.

In this paper, we analyze the effect of the DSD variability on the precision of radar adjustment/calibration by rain gage, by disdrometer, and by polarimetry. These calibration methods are applied in the McGill operational S-band polarimertic radar. ''Gage'' information is derived from a disdrometer. Thus, hereafter when refer to ''gage'' we mean rain rate derived from disdrometer DSDs. The quality of our radar data are relatively poor because of the fast scanning rate (six rotations per minute) and ground echo contamination. Although our disdrometers are relatively close to the radar (within 30 km), the radar-disdrometer comparison is far from an ideal situation due to ground echo contamination. Radar measurements are taken at a location that is above the ground (0.6—1.2 km) and that is shifted from the disdrometer in range and azimuth to minimize ground clutter contamination. Thus, we are in a situation that has some limitations of an operational radar and far from the ideal research radar set-up. However, we still consider a situation at near ranges so that limitations caused by beam filling and shielding at far ranges should be taken into account when a radar-disdrometer comparison is performed at far ranges. Only rain events are considered and bright band contamination is avoided. The effect of inhomogeneous beam filling is minimized by choosing stratiform events in the radar-disdrometer comparison although this effect can be significant in polarimetric calibration. We also investigate the consistency of calibration results obtained with disdrometer and polarimetry, and evaluate an improvement in rainfall estimation with radar reflectivity when radar adjustment or calibration is applied.

The next section describes the influence of the DSD variability on the precision of radar adjustment by comparing radar derived rain rates with those obtained by a rain gage. In this section radar and gage data are simulated from a dis-

drometric data set. Thus, we are isolating only the impact of DSD variability in radar adjustment. In ''Radar calibration by disdrometer-radar comparison'' section, a direct comparison of disdrometer data and actual radar measurements are made and the effect of derived calibration error on rain estimation is investigated. In ''Radar calibration by polarimetry'' section, we discuss a polarimetric calibration method and its theoretical limit due to the variability of DSDs. The sensitivity to the drop deformation is described and the comparison of polarimetric calibration with disdrometric calibration is made.

## Theoretical limit in radar adjustment with a gage due to the DSD variability

The average backscattered received power, $\overline{P}_r$ from the weather targets is $\overline{P}_r = C\frac{Z_e}{r^2}$, where $Z_e$ is the radar reflectivity factor, $r$ the distance from the radar to the weather targets, and $C$ is the radar constant. The latter is a function of radar and path characteristics including the transmitted power, beam width, antenna gain, frequency, radome attenuation, etc. The above equation is written in a different form as

$$Z_e\ (\mathrm{dBZ}) = 10\log\overline{P}_r + 20\log r + C', \tag{1a}$$

where $C' = -10\log C$, the radar constant in dB, and this constant must be obtained by radar calibration. $Z_e$ (dBZ) can be calculated from the average received power when the radar constant is obtained by the careful measurement of the various components of the radar system. However, the accurate determination of the radar constant is quite complex.

The many radar-raingage comparisons (Brandes, 1975; Wilson and Brandes, 1979; Koistinen and Puhakka, 1984; Krajewski and Ahnert, 1986; Krajewski, 1987) are widely used in operations and usually referred to as an ''adjustment'' rather than a calibration because of the several sources of errors in the comparison that is not related to the stability of radar system. In the simpler version of the method, observed radar reflectivities are transformed into rainfall rates, using a single or several $R$–$Z$ relationships $Z = aR^b$, and these rates are compared to rainfall rates observed by one or several rain gages. The relevant equation is then

$$\log R_T = \frac{1}{b}\log(r^2\overline{P}_r) + C'', \tag{1b}$$

where $C'' = (C' - 10\log a)/(10b)$ and $R_T$ is the radar transformed rain rate. Radar measurements are volume integrals (with a beam weighting average and post-detection integration), taken at a certain height above ground. These characteristics, coupled with the fine structure of precipitation patterns, make $R_T$ comparison with gages values difficult (even if there is no ground clutter and bright band contamination), and Zawadzki (1975) discussed the inherent errors. These errors will be less severe if the comparison is made at short ranges and on averages over a long period. Thus, we will only consider daily averages.

In this section, we simulate ''gage'' and ''radar'' measurements from 1-min disdrometric data for five years measured by precipitation occurrence sensing system (POSS: Sheppard, 1990). POSS is widely validated as rain gage as well as a disdrometer by comparing it with other disdrometers and gages (Sheppard and Joe, 1994; Campos and Zawadzki, 2000; Miriovsky et al., 2004). Although the sampling volume of POSS ($0.3$–$190\ \mathrm{m^3\ s^{-1}}$ depending on diameter) is three orders of magnitude larger than that of a conventional disdrometer, it is still significantly smaller than that of radar. However, we ignore in this section the problems related to the spatial sampling and assume that the scanning radar and gage see the same DSDs and adjust ''radar'' values in (1b) to ''gage'' values, both obtained from disdrometer data. We assume a disdrometer to be an ideal gage and an ideal radar. The only source of error considered is the variability of the drop size distributions, thus, quantifying the effect of DSD variability in radar adjustment with a gage. However, in this simulation, we assume that the DSD variability in the POSS sampling volume is identical to that in the radar measurement volume. In fact, the DSD variability is scale dependent (Joss and Gori, 1978; Steiner and Smith, 2004; Lee and Zawadzki, 2005a,b) although the DSD variability within a radar measurement volume has not fully investigated. To minimize the scale dependence of the DSD variability due to the different sampling volumes of the radar and disdrometer, we quantify the DSD variability over a sufficiently long period such as the daily scale.

The radar adjustment with gauge can be done in two ways:

(i) Transform instantaneous reflectivities into rain rates and average these on a daily basis for comparison with gage averages. This is the usual procedure;
(ii) Transform daily averages of reflectivity into daily averages of rain rate and compare these with gage averages. This procedure is based on the fact that averages of $Z$ and $R$ are related by the average DSD.

$$Z_{avg} = \int_D D^6[N(D)]_{avg}\,dD \quad \text{and}$$
$$R_{avg} = 6\pi\times10^{-4}\int_D v(D)D^3[N(D)]_{avg}\,dD, \tag{2}$$

where $N(D)$ ($\mathrm{m^{-3}\ mm^{-1}}$) is the number of drops within a unit volume and diameter interval $dD$ (mm) and $v(D)$ ($\mathrm{ms^{-1}}$) is the terminal fall velocity for a given diameter $D$ (mm). The $N(D)$ is measured every minute. The subscript ''avg'' indicates an average over time, over space, or over an interval in reflectivity. Thus, daily averages of $R$ and $Z$ can be derived from daily average DSDs with (2) or by averaging all 1-min values within a day. Since average distributions may be more stable, the second method may be affected by smaller errors, that is, a $R_{avg}$–$Z_{avg}$ relationship may be preferable to an average $R$–$Z$ relationship. A radar calibration based on (ii) is particularly appropriate if it is applied for a long time period. As has been repeatedly shown, long term averaged DSDs for weak to moderate rain rates converge to the form of Marshall and Palmer (1948). In the limit the $R_{avg}$–$Z_{avg}$ relationship becomes deterministic.

To test the second method applied on a daily basis, we first calculate the average DSD ($[N(D)]_{avg}$) for each day from measured 1-min DSDs, $N(D)$ ($\mathrm{m^{-3}\ mm^{-1}}$). Then, average reflectivities ($Z_{avg}$) and rain rates ($R_{avg}$) are calculated using (2). Rain rates less than 0.1 mm $\mathrm{h^{-1}}$ are not included. The scattergram in Fig. 1a shows the result of these computations. The data

used here correspond to 60 days of observations taken during the years 1994 and 1997–2000 by the POSS. Only the days (47 days) that the duration of rain is longer than an hour are shown.

The best fitted relationship for the daily averages is $Z_{avg} = 336R_{avg}^{1.45}$. (Note that although the $R$ vs. $Z$ regression is always done we express it in the more customary $Z - R$ form but call it $R$–$Z$ relationship.) The standard deviation (SD), the average fractional error (AFE) and the standard deviation of the fractional error (SDFE) were calculated by the following equations:

$$\mathrm{SD} = \left[\frac{1}{k}\sum (R_{avg} - R_T)^2\right]^{1/2},$$
$$\mathrm{AFE} = \frac{1}{k}\sum \frac{|R_{avg} - R_T|}{R_{avg}}, \quad (3)$$
$$\mathrm{SDFE} = \left[\frac{1}{k}\sum \left(\frac{(R_{avg} - R_T)}{R_{avg}}\right)^2\right]^{1/2},$$

where $k$ (=47) is a number of data points, $R_{avg}$ is the rainfall rate calculated by the average DSD of day $k$ and $R_T$ is the transformed rainfall rate from the calculated reflectivity of the average DSD using a $R_{avg}$–$Z_{avg}$ relationship (in this case $Z_{avg} = 336R_{avg}^{1.45}$).

Fig. 1b shows the result for the first method. The following steps are performed:

(1) Reflectivities derived from measured 1-min DSDs are transformed into $R_T$ with a climatological $R$–$Z$ relationship $Z = 210R^{1.47}$.
(2) Daily average of $R_T$ (average $R_T$: $y$-axis) is derived for each day.
(3) Rainfall rates ($R$) are calculated from observed 1-min DSDs and then averages of these 1-min $R$ ($R_{1,avg}$: $x$-axis) are obtained. $R_{1,avg}$ and $R_{avg}$ are mathematically equivalent so that we use only the $R_{avg}$ hereafter.

The climatological relationship $Z = 210R^{1.47}$ was obtained from five years (60 days) of POSS data (Lee and Zawadzki, 2005a,b). The differences in errors between the two methods are marginal.

In addition, it is interesting to compare two $R$–$Z$ relationships ($Z = 210R^{1.47}$ and $Z_{avg} = 336R_{avg}^{1.45}$) used for the transformation in Fig. 1a and b. Although the exponents of the relationships are similar, the coefficients are significantly different, resulting into around 2 dB difference in $Z$. The difference in deriving two relationships is the timescale of $R$ and $Z$. Thus, this underlines the fact that climatological $R$–$Z$ relationships depend on the time scale of the DSDs: 1 min average ($Z = 210R^{1.47}$) and daily average ($Z_{avg} = 336R_{avg}^{1.45}$) in Fig. 1a, respectively. This has been already explored in Gosset and Zawadzki (2001).

The effect of day-to-day (or storm-to-storm) variability of DSDs is well illustrated by Fig. 1. Values of $Z$ and $R$ for each point were calculated by the daily average of DSD from POSS data. Therefore, each point reflects the daily ''mean'' microphysics responsible for the rain formation. In other words, the scatter with respect to the best fitted line in Fig. 1a represents the deviation of the daily ''mean'' microphysics from the climatological ''mean'' microphysics. We can hence estimate from Fig. 1 the effect of day-to-day variability of the DSDs (or of the microphysical processes) on the radar adjustment with a gage *if a single R–Z relationship is used*. Based on the above results, the day-to-day variability of the DSDs leads to SD = 0.82–0.84 mm h$^{-1}$, AFE = 21–28%, and SDFE = 28%. Most cases have error below 56% (twice the of SDFE) in radar adjustment with a gage on a daily basis.

These results establish the uncertainty in the determination of the adjustment biases with gages due to the DSD variability alone. Depending on the degree with which the $R$–$Z$ relationship can be determined for each day, the error in adjustment by a single gage will be less than ~56% (twice of SDFE) for most cases. The narrowing down of the DSD for the day can be done by a broad classification of the situation, such as stratiform and convective, or by a more refined classification using polarimetric radar data, if available. However, when a disdrometer is used to calibrate a radar, this uncertainty is not expected. In other words, the DSD variability does not affect the accuracy of the radar calibration error with a disdrometer since no transformation from $Z$ into $R$ with an a priori relationship is required.

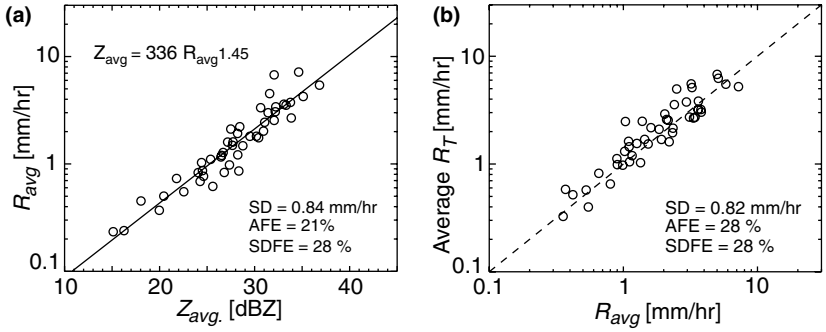


**Figure 1** (a) Scatter-gram of daily averaged rain rate ($R_{avg}$) and reflectivity factor ($Z_{avg}$) derived from daily average DSDs with (2) for 47 days. The best-fit ($Z = 336R^{1.45}$) for these daily averages is shown as solid line. (b) Scatter-gram of daily averaged rain rates obtained after transformation from 1-min $Z$ to 1-min $R$ and actual daily averaged rainfall rates. $Z$ is first calculated from 1-min DSDs and then these calculated reflectivities are transformed into $R$ with the climatological $R$–$Z$ relationship $Z = 210R^{1.47}$ to derived daily average (average $R_T$: $y$-axis). The values on the $x$-axis are the daily average of rainfall rates obtained from 1-min DSDs and are mathematically same as $R_{avg}$ in (a) [see (2)].

## Radar calibration by disdrometer-radar comparison

### Disdrometer-radar comparison

We now compare the reflectivities calculated by the disdrometer with the reflectivities observed by our S-band radar ($\lambda$ = 10.4 cm) and evaluate the possibility of using a disdrometer for a daily calibration of a radar.

At the time of the measurements used here the POSS operated by McGill University was located on the roof of a building in the Montreal downtown campus some 29.3 km to the east-northeast (at 72° azimuth) of the McGill S-band radar. The proximity of Mount Royal, that rises to a height of close to 200 m just to the northwest of the POSS location, produces ground clutter on the S-band radar up to a 1.5 km CAPPI. The closest clutter-free data that can be used for the radar-disdrometer comparison are at 75° azimuth and at a range of 32 km from the radar. Thus, the horizontal distance between the center of the McGill radar measurement box and the POSS location is ~3 km. Thus, our setup is far from ideal and some of the uncertainties in disdrometer-radar comparison may be due to the difference in location of the two measurements. To minimize this problem the comparison between the two instruments is done only on stratiform cases.

Moreover, the S-band radar is not electronically calibrated on regular basis. During the period of these measurements (1999) the radar was in the process of modification for polarization diversity, and afterwards (during the year 2000) affected by a series of transmitter problems. All this conspired against the stability of the system. Fortunately, the use of a linear receiver reduces the calibration problem to one parameter.

An example of the radar-disdrometer comparison is shown in Fig. 2 with different degree of filtering. In Fig. 2a, disdrometer $Z_v$ is derived from 1-min DSDs using a scattering model of Mishchenko et al. (2000) and then is averaged over 10 min. Radar $Z_v$ is the one observed at the height of 1.2 km at the closest clutter free position. To synchronize the time series of radar and disdrometer observations, we calculate the cross-correlation between radar-disdrometer observations and shift according to the time lag of maximum correlation. The asterisks indicate the average of radar reflectivity from 1.2 to 3 km obtained with Gaussian-beam weighting.

In Fig. 2b the radar reflectivities are averaged within a $4 \times 4$ km$^2$ area, leading to a decrease in scatter compared with 1 km resolution. The correlation between the disdrometer and radar $Z_v$ values is excellent. Since the radar was not calibrated, the bias is not surprising. Based on these results, if we neglect the change of the reflectivities below 1.2 km and use the disdrometer as the ground reference, the radar calibration can be performed by increasing $C'$ in (1). In this case, the radar $Z_v$ has to be increased by 1.8 dB (mean bias or radar calibration error = −1.8 dB). This calibration error is derived from the offset between radar and disdrometer $Z_v$ in Fig. 2b (circles) and is indicated by the large circle in Fig. 2c.

Fig. 2a and b shows that we should be careful with real time radar calibration. A comparison between the radar and disdrometer reflectivities within short periods (a comparison of a few points in the figure) can cause a calibration error of 5 dB or more. This large scatter is contributed from the difference in sampling volume, the variation of short-term vertical profile of reflectivity between radar measurement height and the ground, measurement noise, and so on. A more stable calibration is obtained if some filtering of DSDs variability and noise is performed. We use here the sequential intensity filtering technique (SIFT), for short SIFT, that is applied to the disdrometer data and that has been shown to effectively eliminates the effect of undersampling and of drop sorting (Lee, 2003; Lee and Zawadzki, 2003, 2005a,b). That is: (1) for a given day, calculate the average DSD within a certain reflectivity interval (2 dBZ in our example); (2) average the observed radar reflectivities for the data paired with the DSDs data used in (1), and (3) compare the average reflectivities from (1) and (2). The result is shown in Fig. 2c (small circles) for the same day as Fig. 2a and b. Here, the radar data have been averaged over an area of 4 km by 4 km at a fixed height of 1.2 km above the disdrometer. Results obtained by Gaussian smoothing over the 1.2−3 km height interval were consistent and therefore not shown. Similar to the disdrometric data analysis (Lee and Zawadzki, 2003, 2005a,b), the scatter is reduced drastically (to less than 2 dB). This reduction illustrates the effectiveness of SIFT in minimizing several sources of errors such as sampling volume and height difference of measurements. However, as illustrated by the remaining scatter, the narrow interval of reflectivity can still cause a large uncertainty in the determination of the radar calibration error. Thus, the radar calibration errors are determined by obtaining the mean bias from these SIFT data. For this case, a derived calibration error is −2.1 dB. This error is consistent with the mean bias (large circle in Fig. 2c) obtained from circles in Fig. 2b without applying SIFT.

Fig. 3 shows similar information for six other days, and the calibration errors (or mean bias) are shown in Table 1. The same symbols as in Fig. 2c are used. The positive (negative) value of radar calibration indicates overestimation (underestimation) of $Z_v$. In all these cases, we were careful to avoid situations where bright band contamination could be a problem as well as convective situations, where strong gradients are expected. Similar to the comparison in Fig. 2c, some scatter still remains after applying SIFT, indicating that in some cases the 2 dBZ interval is not sufficient to filter out all scatter and to derive a stable calibration error independent of reflectivity values. The difference between the biases with and without applying SIFT in 2 dBZ interval is marginal (see Table 1). Therefore, hereafter, all radar calibration errors are determined from the mean bias of SIFT data. The calibration error in Table 1 varies case to case in the range of −2.7−3.2 dB, indicating some instability of radar.

When applying this disdrometric radar calibration, some constraints are recommended. Due to the contamination by ground clutter and measurement noise, reflectivity larger than 20 dBZ should be used. Numerous data analyses show that a stratiform rain for at least 2−3 h is optimal to ensure an uncertainty of less than 1 dB. When a conventional disdrometer such as Joss−Waldvogel disdrometer is used

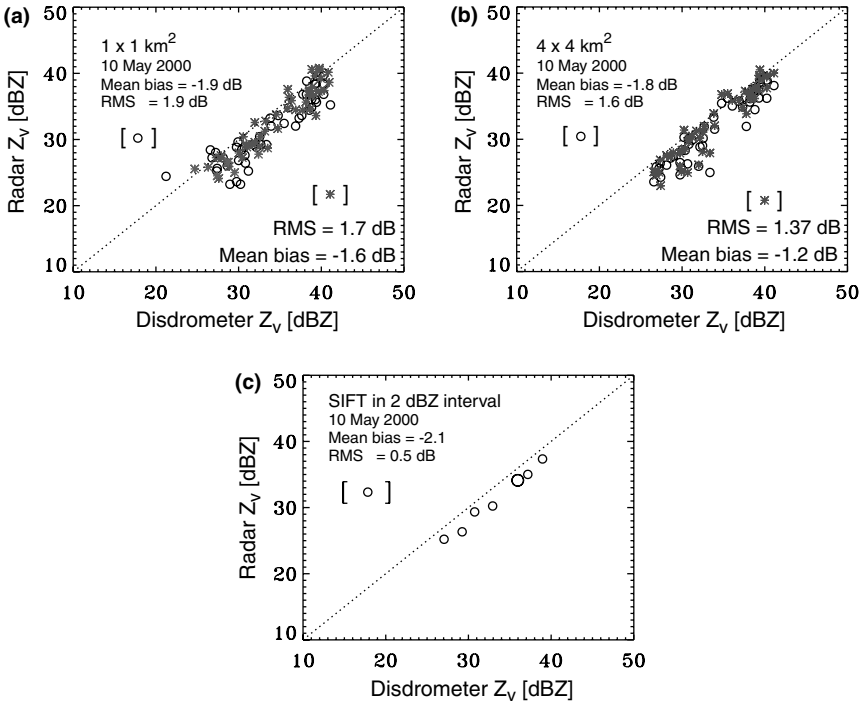


**Figure 2** Scatter-grams of radar measured vertical reflectivities (radar $Z_v$) versus 10 min averages of disdrometer vertical reflectivities (Disdrometer $Z_v$). Circles indicate radar data at 1.2 km height and asterisks are for radar data averaged in height from 1.2 to 3 km. In (a) radar data were taken over 1 km$^2$ and over $4 \times 4$ km$^2$ in (b). Disdrometer $Z_v$ is derived from 1-min DSDs with the scattering model by Mishchenko et al. (2000) and then is averaged in 10 min. (c) Same as (b) after applying the sequential intensity filtering technique (SIFT) with 2 dBZ intervals to daily DSD data. The large circle indicates average $Z_v$ from radar and disdrometer data (circles) in (b). The mean bias [$=1/n\sum$(Radar $Z_v$ − Disdrometer $Z_v$)] indicates the calibration error. The root mean square (RMS) [$=\{1/n\sum$(Radar $Z_v$ − Disdrometer $Z_v$ − Mean bias)$^2\}^{1/2}$] shows the uncertainty in the derived calibration error.

instead of POSS, a larger measurement noise is expected due to a small sampling volume and the difference in the DSD variability caused by different sampling scales of radar and disdrometer should be magnified. Thus, a longer storm duration and stronger rain would be required.

## Consistency of calibration errors derived from two independent disdrometers

Radar-disdrometer comparison can be affected by several sources of errors: height difference between the two measurements, sampling volumes, possible bright band (BB) contamination by side-lobe, possible mis-calibration of POSS, non-uniform beam filling and so on. In ''Disdrometer-radar comparison'' section, we assumed these errors to be small so that radar-disdrometer comparisons can be used as a tool for ''radar calibration.'' However, when these sources are dominant, results of the comparison can only be termed a ''radar adjustment.'' To avoid these possible error sources, radar calibration errors are only determined by averaging radar and disdrometer measurements over a time period of a day.

In this section, we examine the consistency of the derived calibration error with two independent disdrometers that are about 15 km apart. One POSS (POSS2: Macdonald campus) is located at a range of 2 km from McGill S-band radar. Some radar reflectivity measurements above this POSS are contaminated by ground echoes which are eliminated using Doppler radial velocity information. An average reflectivity is computed for an area of 4 km by 4 km centered at a range of 3 km and a height of 1 km. The other POSS (POSS1: Dorval airport) is located at 15 km range from the radar. Radar reflectivities that are used for the comparison with POSS1 are taken from average values within an area of 4 km by 4 km centered at a height of 0.6 km and range of 15 km. Reflectivities from the two POSSs are averaged with 10-min moving windows.

Table 2 shows calibration errors derived from the disdrometer-radar comparison with the two POSSs. Although radar measurement volumes and heights of the comparison are distinctively different, the consistency between the two disdrometer-radar comparisons is remarkable for a given day (see the third and fourth column in Table 2). The absolute difference between the two does not exceed 0.8 dB and, average to only 0.5 dB. The difference in calibration errors is marginal (not shown here) when various radar measurements at different heights below 1.2 km are used. Thus, these results illustrate that this disdrometer-radar comparison method is not significantly affected by the several sources of errors. Furthermore, these results support our claim that this method provides an ''absolute radar calibration'' rather than simply a ''radar adjustment.'' The consistency with polarimetric calibration method described

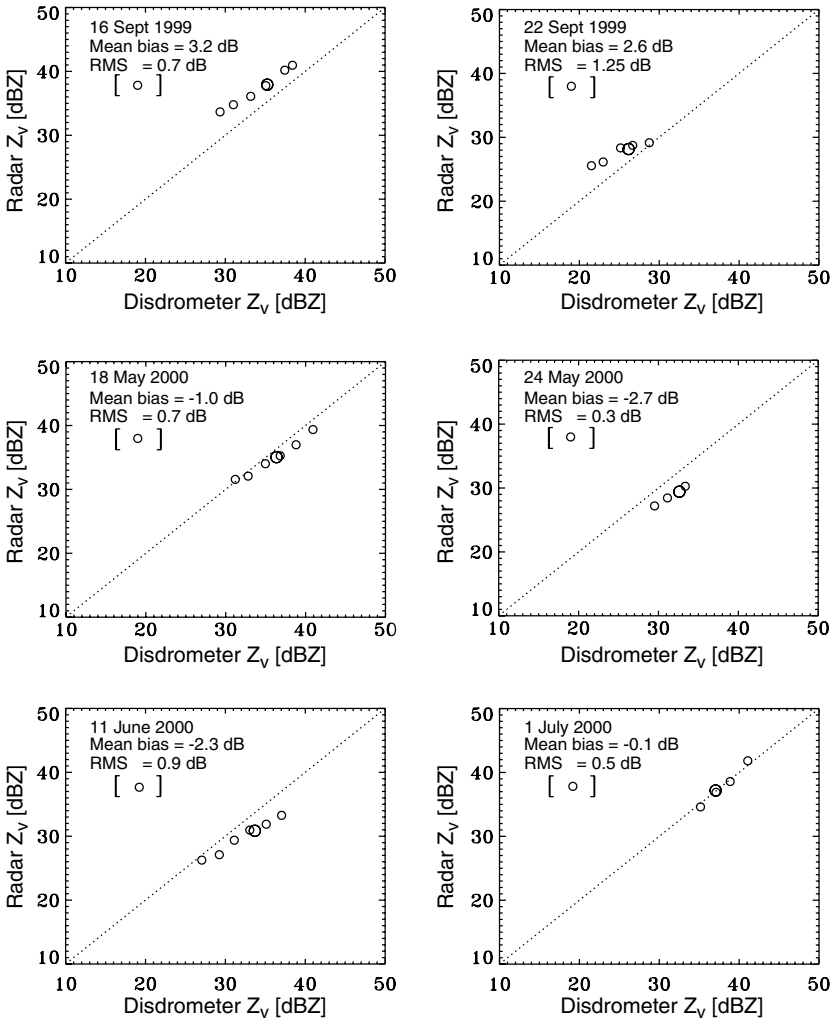


**Figure 3** Six cases of a comparison between $Z_v$ from a scanning radar and $Z_v$ computed from drop size distributions as in Fig. 2c. Before comparison, radar is calibrated with the average bias (2.7 dB) of all cases. The symbols are the same as in Fig. 2c.

**Table 1** Changes in the calibration error (mean bias in dB) as estimated from the radar-disdrometer comparison for the days in Figs. 2c and 3

| Period (UTC) | Calibration error | |
|---|---|---|
| | With SIFT (○) | Without SIFT (◯) |
| 1999. 9. 16. 21:20—1999. 9. 17. 03:20 | 3.17 | 2.68 |
| 1999. 9. 22. 17:50—1999. 9. 22. 23:50 | 2.56 | 1.99 |
| 2000. 5. 10. 19:35—2000. 5. 10. 23:50 | −2.11 | −1.84 |
| 2000. 5. 18. 09:50—2000. 5. 18. 14:50 | −1.04 | −1.32 |
| 2000. 5. 24. 06:50—2000. 5. 24. 14:50 | −2.69 | −3.19 |
| 2000. 6. 11. 21:55—2000. 6. 12. 05:55 | −2.30 | −2.84 |
| 2000. 7. 1. 20:49—2000. 7. 2. 01:49 | −0.08 | 0.12 |

Calibration errors in the second and third columns are the mean bias between radar and disdrometer $Z_v$ with and without applying sequential intensity filtering technique (SIFT) in 2 dBZ intervals, respectively. The symbols (small and big circles) match those in Figs. 2c and 3. The positive (negative) value indicates an overestimation (underestimation) of radar $Z_v$.

in ''Radar calibration by polarimetry'' section further supports this point because the polarimetric calibration is self-consistent.

## Improvement in rain estimation by disdrometric radar calibration

In the previous sub-sections, we estimated the radar calibration error with radar-disdrometer comparison and showed the consistency in the calibration errors derived with two disdrometers independently. Obviously, radar mis-calibration provides a bias in rain estimation, by about 50% error with 3 dB calibration error and by a factor of two with 5 dB error. Hence, the careful monitoring of radar calibration with a disdrometer will reduce errors in rain estimation. We now evaluate the effects of disdrometric radar calibration in hydrological sense.

For the cases in Table 2, POSS1 is now used to calibrate the radar and POSS2 is used as a rain gage. The disdrometric calibration is applied on a daily basis by subtracting the calibration error (the value of the third column in Table 2) from

**Table 2** Changes in the radar calibration error (mean bias in dB) as estimated from the radar-disdrometer comparison with two POSSs for 12 days using SIFT

| # | Period (UTC) | Calibration error (dB) | | $\overline{R}$ (mm h$^{-1}$) | | $\overline{Z}_v$ (dBZ) | | Hours when $Z_v > 10$ dBZ | |
|---|---|---|---|---|---|---|---|---|---|
| | | POSS1 (Dorval airport) | POSS2 (Macdonald campus) | POSS1 | POSS2 | POSS1 | POSS2 | POSS1 | POSS2 |
| 1 | 2002. 5. 30. 02:20–1220 | 0.5 | 0.0 | 3.7 | 3.7 | 27.4 | 28.6 | 5.8 | 5.2 |
| 2 | 2002. 5. 31. 10:00–23:00 | 0.2 | −0.2 | 7.5 | 5.2 | 28.0 | 28.6 | 5.3 | 4.6 |
| 3 | 2002. 6. 15. 14:44–22:44 | 2.4 | 3.1 | 3.3 | 2.0 | 29.2 | 26.9 | 7.8 | 7.8 |
| 4 | 2002. 7. 8. 21:35–23:35 | 5.6 | 6.1 | 0.8 | 1.2 | 21.5 | 24.4 | 0.8 | 1.0 |
| 5 | 2002. 9. 15. 05:52–09:52 | 2.5 | 3.3 | 2.6 | 1.3 | 26.5 | 24.8 | 3.4 | 3.6 |
| 6 | 2002. 9. 23. 02:40–07:40 | 1.5 | 2.1 | 3.3 | 2.9 | 27.9 | 27.5 | 2.7 | 3.3 |
| 7 | 2003. 9. 16. 06:30–10:30 | 4.7 | 4.5 | 0.6 | 0.4 | 17.0 | 17.3 | 1.7 | 1.5 |
| 8 | 2003. 9. 23 04:18–11:18 | 3.3 | 3.6 | 2.7 | 1.8 | 26.0 | 25.7 | 6.2 | 6.8 |
| 9 | 2003. 9. 25. 13:10–17:10 | 3.8 | 3.1 | 0.9 | 1.1 | 21.2 | 23.9 | 2.6 | 3.0 |
| 10 | 2003. 9. 28. 02:40–18:40 | 5.0 | 5.8 | 3.9 | 2.5 | 28.4 | 27.6 | 8.6 | 6.9 |
| 11 | 2003. 10. 15. 05:20–21:20 | 3.0 | 3.2 | 1.6 | 2.2 | 25.5 | 27.2 | 3.9 | 14.8 |
| 12 | 2003. 10. 21. 12:00–17:00 | 1.0 | 0.6 | 2.0 | 3.3 | 24.7 | 27.3 | 3.8 | 4.8 |

Average rainfall rate ($\overline{R}$) and average reflectivity ($\overline{Z}_v$) are also shown for each POSS when the disdrometer measured $Z_v$ is greater than 10 dBZ.

observed radar $Z_v$. The cases in Table 2 have a variety of different characteristics such as the different bright band height and thickness, convection, and drizzle. Three cases (#2, #6, and #10) that are dominated by intermittent periods of precipitation are not used to avoid the effect of non-uniform beam filling. In Fig. 4, radar $Z_v$ is an average in an area of 4 km by 4 km centered at 3 km from the radar and at a height of 1 km and disdrometer $Z_v$ is 10-min average. Fig. 4a shows a $R$–$Z$ scatter plot from POSS2 that is located at 2 km from the radar. All statistics are taken with respect to the climatological $R$–$Z$ relationship $Z = 210R^{1.47}$. This diagram illustrates the variability of DSDs. SDFE = 65% and $r = 0.86$. These are the theoretical limit of rain measurement with a single $R$–$Z$ relationship. However, in addition to the physical variability of drop size distributions, disdrometric measurements are affected by spurious variability because of small sampling volume and drop sorting (Smith et al., 1993; Joss and Zawadzki, 1997). Although undersampling uncertainty in POSS is low because of its large sampling volume (three orders of magnitude larger than conventional disdrometers), nevertheless some spurious variability that is not expected in radar measurements is present (Lee and Zawadzki, 2005a,b). Thus, the statistics should be considered as a combination of physical variability of DSDs and of spurious variability. In Fig. 4b, reflectivities are actual radar measurements. SDFE and AFE are more than twice the variability of DSDs and the correlation $r$ is 0.76. Disdrometric radar calibration is not applied. Hence, this diagram reflects all discrepancies between radar and gage measurements. The large discrepancy can be explained by the radar mis-calibration in addition to all other sources of errors in the gage-radar comparison. After applying a calibration correction on a daily basis, SDFE decreases from 150% to 77% and AFE from 108% to 51% (Fig. 4c). Almost half of the variability is reduced by radar calibration only. The scatter is only slightly larger than that of the variability of DSDs. In addition to the several sources of errors in the comparison, the spatial variability of precipitation should explain a significant portion of the differences in the degree of the scatters in Fig. 4a and c since radar data are taken at location 1 km horizontally apart from the disdrometer. Nevertheless, these results show that the DSD variability is the dominant factor of the scatter in Fig. 4c.

Instead of disdrometric radar calibration, radar reflectivity can be adjusted with a rain gage as described in ''Theoretical limit in radar adjustment with a gage due to the DSD variability'' section. A radar daily rain accumulation is estimated from radar measured $Z_v$ using the climatological $R$–$Z$ relationship $Z = 210R^{1.47}$ and is compared with an accumulation derived from POSS1 to derived a daily radar adjustment bias. Similar to Fig. 4c, this bias is applied to adjust the radar measured $Z_v$. Fig. 4d shows the scatter plot of disdrometer $R$ from POSS2 versus radar adjusted $Z_v$. In contrast with the disdrometric radar calibration in Fig. 4c, the scatter shows large outliers and the mean bias is not eliminated completely. SD = 2.2 mm h$^{-1}$, SDFE = 117% and $r = 0.79$. These large errors are a consequence of using a single $R$–$Z$ relationship to adjust radar measurements instead of proper relationship for a given day. In other words, the day-to-day DSD variability is not taken into account properly and, as described in ''Theoretical limit in radar adjustment with a gage due to the DSD variability'' section, this is a significant factor that causes large error in the radar adjustment with gage.

Noise due to disdrometer undersampling increases the scatter in $R$–$Z$ plot and results in a spurious relationship when the error in both variables is not taken into account in the regression (Amemiya, 1997; Lee and Zawadzki, 2005a,b). However, when the method of weighted total least squares (WTLS) regression which takes into account the errors in $R$ and $Z$, the derived relationship is close to the true one (Amemiya, 1997; Davis, 1999).

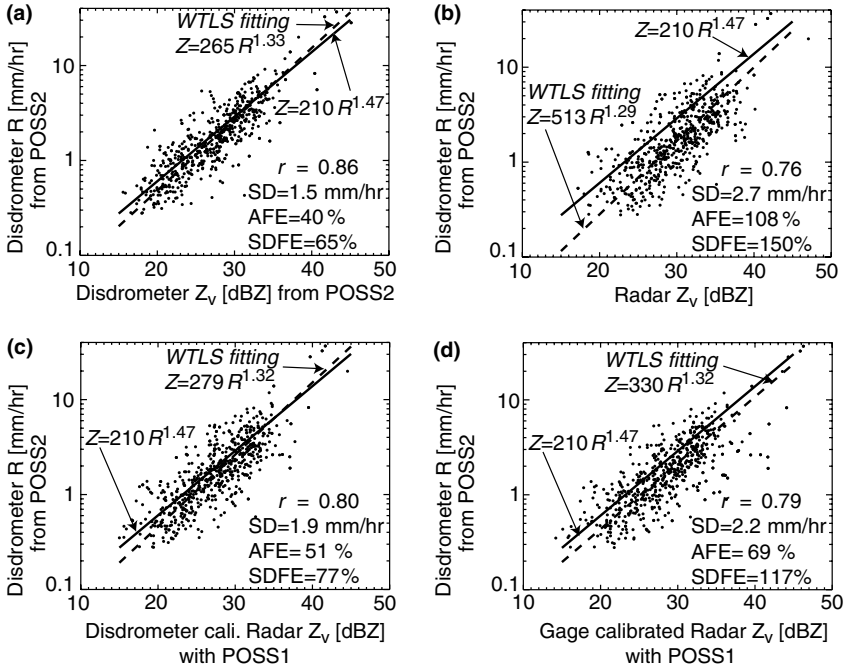


**Figure 4** (a) $R-Z_v$ scatterplot from disdrometric data (POSS2) for nine days of rain during the years 2002 and 2003. Both $R$ and $Z_v$ are 10-min average. The disdrometer (POSS2) is located 2 km from radar. (b) $R$ from POSS2 and radar $Z_v$ taken from an average over $4 \times 4$ km$^2$ area centered at 3 km in range and 1 km above the ground. Radar data that are affected by ground echoes are eliminated prior to the average. (c) Same as in (b) but after a daily radar calibration obtained from a radar-disdrometer comparison using POSS1 located 15 km from radar. (d) Same as in (b) but after applying a daily radar adjustment obtained with radar-gage comparison using POSS1 as a rain gage. $r$ is the correlation coefficient. All statistics are taken with respect to the climatological relationship $Z = 210R^{1.47}$ that is indicated by the solid line. The dashed lines indicate the best weighted total least squares (WTLS) fitting for given pairs of $R$ and $Z_v$.

From the pairs of $R$ and $Z_v$ in Fig. 4, $R-Z$ relationships are derived using WTLS. The derived relationship from disdrometric data are $Z_v = 265R^{1.33}$. The exponent (coefficient) is smaller (larger) than that of the climatological $R-Z$ relationship due to the limited data set. When $Z_v$ from radar is used to avoid the undersampling effect in Fig. 4c, a similar relationship ($Z_v = 279R^{1.32}$) is derived after applying the radar calibration. Thus, results show that the $R-Z$ relationship derived from our disdrometric data are not affected by the undersampling and can be used in radar rain estimation by minimizing the effects of the DSD variability. Furthermore, the derived relationship follows the power law relationship that is consistent with the original power-law form by Marshall and Palmer (1948) who derived the relationship with a very limited sampling size. This power law is related to the scaling properties of observed DSDs (Lee et al., 2004). Before applying the disdrometric radar calibration, the pair of (DSD $R$, radar $Z_v$) provides the similar exponent of $R-Z$ relationship ($Z_v = 513R^{1.29}$). The mean radar calibration error is included in the large coefficient.

## Radar calibration by polarimetry

Additional information from polarimetry has been applied in rain estimation to reduce the effects of the variability of drop size distributions. Gorgucci et al. (1992) suggested a radar calibration technique with polarimetry that calculates the calibration error by comparing estimated $R$ from ($Z_h$, $Z_{DR}$) and $K_{DP}$. The former rain estimator is affected by radar calibration whereas the latter is independent of it. Therefore, the radar calibration can be achieved by adjusting the radar calibration offset to have an agreement in rain estimation from both estimators. However, polarimetric data are affected by large statistical uncertainty (Doviak and Zrnic, 1993) and rain estimation solely from polarimetric data are still debatable. In particular, the statistical uncertainty is larger in a fast scanning operational radar. Hence, the use of an integrated parameter such as $\Phi_{DP}$ rather than $K_{DP}$ is preferable in seeking to reduce the uncertainty in radar calibration.

In this section, we investigate the effect of the variability of drop size distributions on the radar calibration with polarimetry. A new radar calibration method using $\Phi_{DP}$ is presented and applied in operational S-band polarimetric radar data.

### Error in radar calibration by polarimetry due to the variability of DSDs

The reflectivity factor is affected by the calibration error while its statistical uncertainty is relatively smaller than that of any polarimetric parameters. The specific differential phase shift $K_{DP}$ is independent of the calibration error since it is a propagation characteristic. The calibration error in differential reflectivity $Z_{DR}$ can be kept within around 0.2 dB by measuring light rain at vertical pointing mode.

Using these facts, the radar calibration can be checked by comparing estimated $R$ from ($Z_h$, $Z_{DR}$) and $K_{DP}$ (Gorgucci et al., 1992). Alternatively, instead of estimating $R$, the radar calibration can be performed by directly estimating one radar measurable parameter from another. First, estimate $Z_h$ from $K_{DP}$, or from ($K_{DP}$, $Z_{DR}$). Then adjust radar calibration offset to have the same measured and calculated $Z_h$. The theoretical limit of this calibration depends on the accurate estimation of one parameter. The accuracy is a function of the variability of DSDs. Using five years of disdrometric data (1994, 1997–2000) measured by POSS, the relationship between $K_{DP}$ and $Z_h$ is derived (Fig. 5a). Radar measurables are calculated from a scattering model (Mishchenko et al., 2000) by assuming the drop deformation of Pruppacher and Beard (1970), a temperature of 10 °C, and wavelength $\lambda$ = 10.4 cm. An excellent correlation is apparent and the effect of DSD variability is small as shown by the small scatter. A least square fit (solid line) in log–log space gives

$$Z_h = 3.95 \times 10^4 K_{DP}^{1.18}, \quad (4)$$

where $K_{DP}$ is defined as the value for one-way. Using this equation, $Z_h$ can be retrieved from $K_{DP}$ accurately and vice versa. This power law is the only necessary information in the polarimetric radar calibration. The scatter around this power law determines the theoretical limit of this radar calibration. In Fig. 5b, the degree of the scatter is provided by the SD in the estimation of $Z_h$ with (4). SD (solid line) is less than 1 dB except for a point at large $K_{DP}$ that is affected by insufficient data. Therefore, the limitation of such a calibration due to the variability of DSDs is about 1 dB. The variability of DSDs can be significantly reduced by adding one more parameter, namely $Z_{DR}$. The limitation is reduced to less than 0.5 dB with $Z_h = 8.79 \times 10^3 K_{DP}^{1.00} 10^{0.447 Z_{DR}}$. Therefore, the effect of the variability of DSDs on this radar calibration is almost negligible.

Now we can consider applying this methodology to an operational polarimetric radar. An important issue is the quality of polarimetric data. Although most research radars use as a guideline a scanning rate of 1 rpm, the fast scanning (6 rpm for McGill S-band radar) is essential for an operational radar to reduce the return time and maximize the volumetric surveillance. Thus, the dwelling time for each pixel (i.e., 1° by 1 km) is relatively short and the number of pulses for each pixel is small. Therefore, the same quality as in slow scanning radars cannot be expected. In addition, $K_{DP}$ is not a direct measurable parameter but a spatial derivative of one-way differential phase shift $\Phi_{DP}$. It is subject to a large uncertainty, particularly if averaged over short distance (1 km). $Z_h$ has less uncertainty than $K_{DP}$. Therefore, it is preferable to estimate $K_{DP}$ from $Z_h$ and use $\Phi_{DP}$ instead of $K_{DP}$. $Z_{DR}$ is not sensitive to the absolute calibration, but is very sensitive to the relative calibration errors between the two channels. These relative calibration errors can arise from a variety of sources associated with physical differences in the $H$ and $V$ transmit and receive paths. Since a $Z_{DR}$ precision of 0.2–0.5 dB is usually required for most applications, small relative calibration errors can contaminate $Z_{DR}$ values. The technique of pointing the radar directly upward during rain (sometimes called birdbaths) where the theoretical $Z_{DR}$ = 0 dB is used by several organizations to address the relative calibration offsets. Unfortunately, our fast scanning S-band operational radar cannot perform this procedure due to its antenna mechanics as well as the operational environment. Thus, $Z_{DR}$ is not properly calibrated. In addition, the measurement noise of $Z_{DR}$ from our fast scanning S-band polarimetric radar is significantly large, that is around 0.33 dB at 1° by 1 km (see Table 6.5 in Lee, 2003). Therefore, only $\Phi_{DP}$ and $Z_h$ are used in our new calibration technique to minimize the effects of measurement errors.

## Procedure

The details of a radar calibration procedure are presented in this sub-section. The procedure is quite similar to the method described by Goddard et al. (1994) except for using $Z_h$–$K_{DP}$ relationship instead of $Z_h$–($K_{DP}$, $Z_{DR}$). Instead of using a single path, a statistical tool that combines a number of paths at several volume scans is used to minimize radar measurement noise. Only rain regions are identified, that is, for each radial the starting polar pixel is the first pixel with precipitation free from ground echo contamination and the last pixel is just before the bright band. The path between these two pixels must not be contaminated by any ground echo or hail. Then, the following procedure is applied:

1. Calculate $K_{DP}$ at every pixel (i.e., every km) along the path from measured $Z_h$ with a known $Z_h = aK_{DP}^b$ in (4).

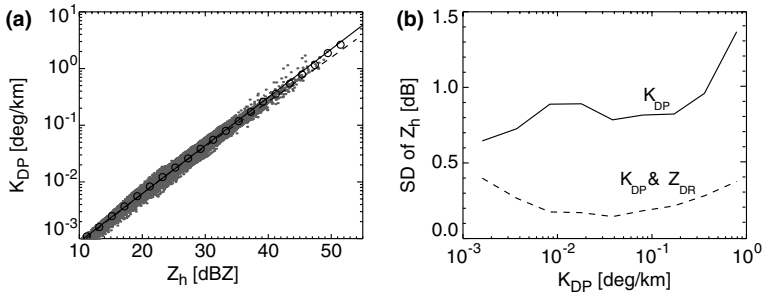


**Figure 5** (a) Scatter-gram of $K_{DP}$–$Z_h$ calculated from five years of disdrometric data. The solid line is the least square fit ($Z_h = 3.95 \times 10^4 K_{DP}^{1.18}$) and the dashed line is from Marshall–Palmer distribution. Circles are $Z_h$–$K_{DP}$ for average DSDs in 2 dBZ interval. (b) The standard deviation in the estimation of $Z_h$ with the climatological relationships $Z_h = 3.95 \times 10^4 K_{DP}^{1.18}$ and $Z_h = 8.79 \times 10^3 K_{DP}^{1.00} 10^{0.447 Z_{DR}}$.

2. Calculate $\Phi_{DP}$ by integrating the calculated $K_{DP}$ along the path.
3. Calculate the slope between calculated and measured $\Phi_{DP}$.
4. Estimate the calibration error $\varepsilon$ from the slope using the following equation:

$$\varepsilon\ (\mathrm{dB}) = 10b\log(\tan\theta), \tag{5}$$

where $b$ is the exponent of $Z_h$–$K_{DP}$ relationship and $\tan\theta$ is the slope of calculated and measured $\Phi_{DP}$ [see Appendix and (6)].

## Analysis

An example of comparison between calculated and measured $\Phi_{DP}$ along one radial at 0.9° elevation angle is shown in Fig. 6a. The dashed lines are the $\Phi_{DP\_cal}$ calculated from $Z_h$ or $Z_h + dZ_h$ using (4). $dZ_h$ may be considered as the assumed calibration error. The measured $\Phi_{DP}$ (thin solid line) is noisy, with fluctuations larger than 1 dB. The variability of DSDs can account for 1 dB, the remaining being due to measurement errors. When $\Phi_{DP}$ is small ($\Phi_{DP} < 3°$), the noise is dominant, implying that our procedure cannot be used. The smooth line (thick solid line) of measured $\Phi_{DP}$ is located between $Z_h - 1$ dB and $Z_h - 2$ dB at $\Phi_{DP} > 3°$. Hence, by subtracting 1 or 2 dB from $Z_h$, $\Phi_{DP\_cal}$ can be adjusted to coincide with the measured $\Phi_{DP}$. Hence, the calibration error is 1 or 2 dB. However, due to the significant noise in the measurement, this adjustment is not reliable as each path gives a different calibration error.

A more robust way of estimating the calibration error is necessary. It can be achieved by extending the data set by including all paths for a storm (4 h). The scatter plot of calculated and measured $\Phi_{DP}$ along the paths in Fig. 6b shows the deviation from 45° line ($\varepsilon = 0$) that indicates a calibration error. When the slope is large than 45°, the radar reflectivity is over-estimated ($\varepsilon > 0$). The slope (solid line) is calculated by the least square fit. The fitted line is forced to pass through the origin. Hence, a formula for the slope is

$$\tan\theta = \frac{\sum \Phi_{DP\_cal}\Phi_{DP}}{\sum \Phi_{DP}^2}. \tag{6}$$

In this case, an overestimation of $\varepsilon = 1.8$ dB derived from (5) and (6). Hence, an offset of 1.8 dB must be applied to the radar calibration. The corrected radar calibration offset should provide the absolute calibration of the radar since the polarimetric calibration is a self-consistent method.

The scatter is quite larger than that expected from the variability of DSDs ($\varepsilon \pm 1$ dB). It is more prominent at small $\Phi_{DP}$ than at large $\Phi_{DP}$. In addition to the effect of the DSD variability, this large scatter may be caused by several reasons: radar measurement noise, inhomogeneous beam-filling, possible bright band contamination, possible variation of drop shape, and so on. As noted by the outliers at small $\Phi_{DP}$ and by their reduction with increasing $\Phi_{DP}$, a significant potion of the large scatter originates from radar measurement noise caused by the fast scanning rate (6 rpm) of the McGill operational S-band polarimetric radar. We expect this scatter should be reduced significantly for most research radars that are operate at a slow scanning rate ($\sim$1 rpm). The effect of bright band contamination is insignificant since data are excluded when the 3 dB edge of the radar beam intercepts the bright band limits. Gorgucci et al. (2001) showed a significant fluctuation of drop deformation that depends on the relative location within the storms (updraft and downdraft regions) and geographical regions. When this fluctuation is considered, some of the large scatter is also contributed from the variation of drop shape. A systematic quantification of the effect of these sources remains as an interesting subject to explore in the future.

More stable results are obtained if pixels with $\Phi_{DP} < 3°$ are eliminated. This scatter also suggests that this technique can lead to large fluctuation of the calibration error unless it is applied for a sufficiently long time. The fluctuation of the estimated calibration errors is examined for various time intervals. Fig. 7 shows the temporal variation of the estimated calibration error for 5 min (one volume scan: circles) and 30 min (six volume scans: solid line) but computed every 5 min. The former shows the fluctuation from −0.2 to 3.4 dB while the latter varies almost within the variability of DSDs (SD = ±1 dB). These results suggest that a data set of at least an hour is required to achieve a stable calibration error. This lower limit depends on the intensity of storm, since the noise becomes less important with increasing intensity. Thus, we suggest that rain echoes lasting for at least an hour with

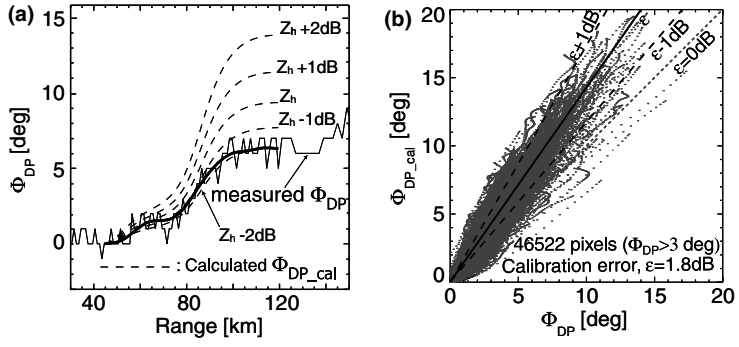


**Figure 6** (a) Comparison of measured $\Phi_{DP}$ (thin solid line) along a path with $\Phi_{DP}$ calculated from $Z_h$ ($\Phi_{DP\_cal}$: dashed lines). The climatological relationships $Z_h = 3.95 \times 10^4 K_{DP}^{1.18}$ is used to calculate $\Phi_{DP}$ from measured $Z_h$. The thick solid line is the smoothed value of measured $\Phi_{DP}$. (b) Scatter-gram of measured ($x$-axis) and calculated ($y$-axis) $\Phi_{DP}$ on 25 September 2001. Solid line is a fitted line and is used to estimate the calibration error ($\varepsilon$). Two long dashed lines represent the possible range of the uncertainty of polarimetric radar calibration due to the variability of DSDs ($\varepsilon \pm 1$ dB).

reflectivity greater than 35 dBZ over at least 10–20° in azimuth and 10–20 km in range are required for the derivation of a stable calibration error.

## Sensitivity to drop deformation

Polarimetric information is a response to the nonspherical shape of drops. More deformed drops provide stronger polarimetric signature. When different formulas of drop deformation are used for the same DSD, the relationship between $Z_h$ and $K_{DP}$ varies. The sensitivity of the polarimetric variables to the drop deformation can result in a significant bias as well as random error in $R$ estimation (Keenan et al., 2001; Lee, 2003). We have assumed the drop deformation formula by Pruppacher and Beard (1970) to calculate radar measurables from DSDs. The literature shows different forms of drop deformation. The following four formulas are widely used to calculate radar measurables from DSDs.

(1) Pruppacher and Beard (1970):

$$e = 1.03 - 0.062D \quad [D \geqslant 0.5\ \text{mm}].$$
$$e = 1 \quad [D < 0.5\ \text{mm}].$$

(2) Illingworth and Johnson (1999):

$$e = 1.0166 - 9.8 \times 10^{-3}D - 0.0252D^2 + 3.75 \times 10^{-3}D^3 - 1.699 \times 10^{-4}D^4 \quad [D > 1\ \text{mm}],$$
$$e = 1 \quad [D \leqslant 1\ \text{mm}].$$

(3) Goddard and Morgan (1995):

$$e = 1.075 - 0.065D - 3.6 \times 10^{-3}D^2 + 4 \times 10^{-4}D^3 \quad [D > 1.1\ \text{mm}],$$
$$e = 1 \quad [D \leqslant 1.1\ \text{mm}].$$

(4) Andsager et al. (1999)

$$e = 1.012 - 0.0144D - 0.0103D^2 \quad [1.1\ \text{mm} \leqslant D \leqslant 4.4\ \text{mm}],$$
$$e = 1.0048 + 5.7 \times 10^{-4}D - 2.628 \times 10^{-2}D^2 + 3.682 \times 10^{-3}D^3 - 1.677 \times 10^{-4}D^4 \quad [\text{otherwise}],$$
$$e = 1 \quad \text{if} \quad e > 1,$$

where $e$ is the axis ratio and $D$ (mm) is the equivolumetric diameter. These four formulas are graphically shown in Fig. 8. The formula by Pruppacher and Beard (1970) gives most deformed drops at $D < 3$ mm and for that of Andsager et al. (1999) drops are least deformed at 1.7 mm < $D$ < 4 mm. Using these four formulas, the relationship between $Z_h$ and $K_{DP}$ is calculated as in (4) and is shown in Table 3. The exponent of the $Z_h$–$K_{DP}$ relationship is within 1.0–1.2 while the coefficient varies more significantly from $4.0 \times 10^4$ to $6.5 \times 10^4$. This inconsistency of the relationships affects the radar calibration. For example, there is a difference of 2 dB in computing $Z_h$ with $K_{DP} = 1^\circ\ \text{km}^{-1}$ from the four different formulas. Using these four formulas, the calibration error is calculated on a daily basis and is shown in Table 4. The difference between Pruppacher and Beard (1970) and Andsager et al. (1999) is about >2 dB that is twice of the variability of DSDs. Therefore, the information on drop deformation is a more important factor than the variability of DSDs. Without knowing the exact drop deformation, the theoretical limit (1 dB) due to the variability of DSDs cannot be achieved.

However, an interesting fact emerges from the comparison of the polarimetric calibration with disdrometric calibration. There is a consistency between the two when the

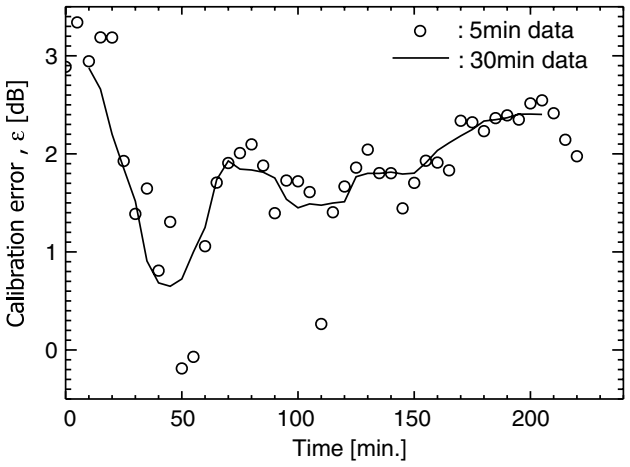


**Figure 7** Time variation of calibration error for two different time windows. Circles are obtained from one volume scan while solid line is from six volume scans.

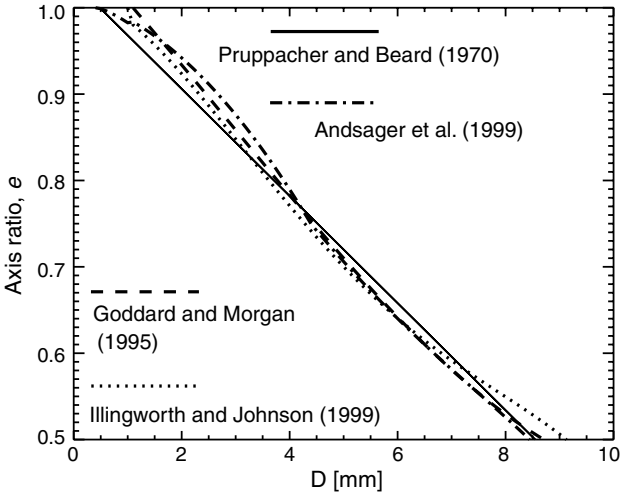


**Figure 8** Graphical illustration of four different drop deformation formulas from the literature.

**Table 3** Coefficient $a$ and exponent $b$ of the relationship $Z_h = aK_{DP}^b$ derived from disdrometric data for five years using four different drop deformation formulas

| Deformation formula | $a$ of $Z_h = aK_{DP}^b$ | $b$ of $Z_h = aK_{DP}^b$ |
|---|---|---|
| Pruppacher and Beard (1970) | $3.95 \times 10^4$ | 1.18 |
| Illingworth and Johnson (1999) | $4.17 \times 10^4$ | 1.01 |
| Goddard and Morgan (1995) | $5.67 \times 10^4$ | 1.03 |
| Andsager et al. (1999) | $6.50 \times 10^4$ | 1.13 |

**Table 4** Radar calibration error $\varepsilon$ estimated from polarimetric technique with four different drop deformations and from disdrometric calibration

| Date | Calibration error, $\varepsilon$ (dB) | | | | |
|---|---|---|---|---|---|
| | Polarimetric calibration with $\Phi_{DP}$ | | | | Disdrometric calibration |
| | 1 | 2 | 3 | 4 | |
| 1999. 9. 16. | 0.7 | −0.7 | −1.9 | −1.7 | 1.4 |
| 2000. 5. 10. | 3.7 | 3.1 | 1.8 | 1.4 | 3.6 |
| 2001. 9. 13. | −2.4 | −3.6 | −4.8 | −4.9 | −1.7 |
| 2001. 9. 25. | 1.8 | 0.4 | −0.8 | −0.7 | 1.5 |
| 2002. 7. 8. | 5.1 | 5.0 | 3.6 | 3.0 | 5.0 |
| 2002. 9. 15. | 3.2 | 2.5 | 1.2 | 0.9 | 3.9 |
| 2002. 9. 23 | 2.9 | 2.2 | 0.9 | 0.6 | 3.5 |

1: Pruppacher and Beard (1970).
2: Illingworth and Johnson (1999).
3: Goddard and Morgan (1995).
4: Andsager et al. (1999).

Pruppacher and Beard (1970) deformation are used. The difference in calibration errors between disdrometric and polarimetric (with Pruppacher and Beard, 1970) calibration is smaller than 0.7 dB. Thus, the difference is within the theoretical limit of 1 dB due to the DSD variability. This consistency indicates the stability of two calibration methods and suggests the possibility of retrieving the mean drop deformation by comparing the two calibration methods. Furthermore, since the polarimetric calibration method provides the absolute calibration of radar, the results illustrate that the disdrometric calibration should be considered as a tool for the ''absolute radar calibration.'' There is still a considerable case to case variation of calibration errors. This is likely due to the instability of our radar.

## Discussions

One rain gage located close to the radar, preferably shielded behind obstacles that would eliminate ground clutter contamination, can be used for radar adjustment on a daily basis. The uncertainty of such an adjustment, due to day-to-day DSD variability alone, can be large with SDFE = 28% if a single DSD is used for the $Z$ to $R$ transformation. This uncertainty should decrease when daily $R$—$Z$ relationships are identified from the other tools. We have simulated radar and gage measurements from DSDs to quantify the theoretical limits. In practice the gage will have also errors and several gages are preferable as long as their location with respect to the radar is optimized. However, when a disdrometer is used for daily radar calibration, the uncertainty due to the DSD variability is removed because no $R$—$Z$ relationship is necessary.

The excellent correlation obtained between radar and disdrometer reflectivity suggests that a single disdrometer can be an excellent alternative for daily radar calibration or for calibration monitoring. Our S-band radar was not calibrated electronically during the period of the measurements used in this study. In ''Improvement in rain estimation by disdrometric radar calibration'' section, we have used one POSS for disdrometric calibration and the other as a rain gage to investigate the effect of disdrometric radar calibration on radar rain estimation. By applying disdrometric calibration for this period we achieved an significant improvement in the estimation of 10-min average rainfall rate: SDFE reduced from 150% to 77% and likewise for AFE (from 108% to 51%).

Even though our disdrometer has a sampling volume that is three orders of magnitude larger than that of other disdrometers, it remains much smaller than that of a typical radar sampling volume. Thus, there may be an issue of representativeness. However, to avoid this issue, we have calculated the radar calibration error over a long time period (a day or an entire storm). Furthermore, the radar-disdrometer reflectivity difference due to their different measurement heights should be filtered out by mixing various situations (i.e., evaporation, low-level growth, etc.) within such a long term. The similar calibration errors derived from two independent POSSs suggests that the disdrometric radar calibration is not significantly affected by these several sources of errors. Disdrometric and polarimetric radar calibration also provides similar calibration errors within 0.7 dB. The input data sets used for disdrometric radar calibration consist of uniform stratiform rain without bright band contamination. In these circumstances, problems of unrepresentativeness, inhomogeneous beam filling, and/or height differences have been compensated. Thus, overall results illustrate that the radar-disdrometer comparison can be used as a tool for an *absolute radar calibration* rather than simply a *radar adjustment*.

In contrast with the disdrometric calibration, the radar calibration by polarimetry is a self-consistent method since it does not need any external reference. Governing factors are the variability of DSDs and noise in measurements. The variability of DSDs limits the accuracy of this method to 1 dB uncertainty. In addition, uncertainty on drop deformation gives an uncertainty of about over 2 dB in calibration. However, for the drop deformation formula of Pruppacher and Beard (1970), the absolute agreement of calibration errors derived from disdrometric and polarimetric radar calibrations suggests the stability of two methods. This agreement can be used to retrieve the information on drop deformation. To guarantee a stable polarimetric radar calibration, at least an hour of intense echoes exceeding 35 dBZ over 10—20° in azimuth and 10—20 km in range is a minimal condition.

It is important to address the calibration issue of POSS. A precise POSS beam pattern was measured in the laboratory for our instrument and DSD retrieval was carefully evaluated with simulation. DSDs from POSS and other disdrometers based on different principles agreed well (Campos and Zawadzki, 2000, as well as additional studies performed during this study).

The agreement between disdrometric and polarimetric calibration seems to indicate that the drop deformation formula of Pruppacher and Beard (1970) is the most appropriate form in our environment. This result is different from the recent trend in the literature that suggests a less deformed formula of drop shape. For our result to be consistent with that from the literature, reflectivity from POSS should increase up to 3 dB in order to decrease radar calibration errors derived from the radar-disdrometer comparison. Based on comparison with the other disdrometers and conventional rain gages, it is unlikely that such

a large error in POSS reflectivity is possible. However, a more in-depth study of POSS calibration and determination of drop deformation by comparing disdrometric and polarimetric calibrations are interesting subjects to explore.

## Acknowledgements

This work was partially supported by a grant from the Canadian Foundation for Climate and Atmospheric Sciences. The authors are indebted to Dr. Aldo Bellon for numerous constructive comments and for editing this manuscript.

## Appendix. The radar calibration error derived from the slope of calculated and measured $\Phi_{DP}$

Here, we derive the relationship between the radar calibration error $\varepsilon$ and the slope of the calculated and measured differential phase shift $\Phi_{DP}$. Let us assume a perfect power law ($Z_h = aK_{DP}^b$) between $Z_h$ and $K_{DP}$, a reasonable approximation of the relationship between $Z_h$ and $K_{DP}$. The one-way differential phase shift $\Phi_{DP}$ is an integration of one-way specific differential phase shift $K_{DP}$.

$$\Phi_{DP} = \int_0^r K_{DP}\,dr = a^{-1/b}\int_0^r Z_h^{1/b}\,dr. \tag{A.1}$$

Since the backscattering phase shift is negligible in S-band radar, the backscattering phase shift is neglected in the current study. With shorter wavelengths, the effect of backscattering phase shift should be explored prior the application of this calibration method. When there are no measurement errors, $\Phi_{DP}$ is the same as the measured $\Phi_{DP}$. Hereafter, we will denote $\Phi_{DP}$ as the measured one. If there is a calibration error $\varepsilon$ in $Z_h$, then the differential phase shift $\Phi_{DP\_cal}$ calculated from $\varepsilon Z_h$ can be written in the following form:

$$\Phi_{DP\_cal} = a^{-1/b}\int_0^r (\varepsilon Z_h)^{1/b}\,dr. \tag{A.2}$$

By comparing (A.1) and (A.2), the calibration can be expressed in terms of the slope of $\Phi_{DP\_cal}$ and $\Phi_{DP}$.

$$\begin{aligned} \varepsilon &= \left(\frac{\Phi_{DP\_cal}}{\Phi_{DP}}\right)^b = (\tan\theta)^b, \\ \varepsilon\ (\mathrm{dB}) &= 10b\log_{10}\frac{\Phi_{DP\_cal}}{\Phi_{DP}} = 10b\log_{10}(\tan\theta), \end{aligned} \tag{A.3}$$

where $\tan\theta$ is the slope of calculated and measured $\Phi_{DP}$. When the slope is calculated from (6), the radar calibration can be directly estimated from (A.3).

## References

Amemiya, Y., 1997. Generalization of the TLS approach in the errors-in-variables problem. In: Van Huffel, S. (Ed.), Recent Advances in Total Least Squares Techniques and Errors-in-Variables Modeling, Stochastic Method in Hydrology, vol. 7. SIAM, Philadelphia, PA, pp. 77–86.

Andsager, K., Beard, K., Laird, N.F., 1999. Laboratory measurements of axis ratios for large rain drops. J. Atmos. Sci. 56, 2673–2683.

Brandes, E.A., 1975. Optimizing rainfall estimates with the aid of radar. J. Appl. Meteorol. 14, 1339–1345.

Campos, E., Zawadzki, I., 2000. Instrumental uncertainties in $Z$–$R$ relations. J. Appl. Meteorol. 39, 1088–1102.

Davis, T.G., 1999. Total least-squares spiral curve fitting. J. Surv. Eng. 125, 159–176.

Doelling, I.G., Joss, J., Riedl, J., 1998. Systematic variation of $Z$–$R$ relationships from drop size distributions measured in northern Germany during seven years. Atmos. Res. 47–48, 635–649.

Doviak, R.J., Zrnic, D.S., 1993. Doppler Radar and Weather Observations. Academic Press, San Diego, CA, 562pp.

Fabry, F., Zawadzki, I., 1995. Long term radar observations of the melting layer of precipitation and their interpretation. J. Atmos. Sci. 52, 838–851.

Germann, U., 2000. Spatial continuity of precipitation, profiles of radar reflectivity and precipitation measurements in the Alps. Swiss Federal Institute of Technology (ETH), Ph.D. Thesis, 104pp.

Goddard, J.W., Morgan, K.L., 1995. Dual-wavelength polarization measurements in precipitation using the camera and Rabelais radars. In: 27th Conference on Radar Meteorology. American Meteorological Society, Vail, CO, pp. 196–198.

Goddard, J.W., Tan, J., Thurai, M., 1994. Technique for calibration of meteorological radars using differential phase. Electon. Lett. 30, 166–167.

Gorgucci, E., Scarchilli, G., Chandrasekar, V., 1992. Calibration of radars using polarimetric techniques. IEEE Trans. Geosci. Remote Sensing 30, 853–858.

Gorgucci, E., Chandrasekar, V., Scarchilli, G., Steve Bolen, 2001. Variation of mean raindrop shape derived from polarimetric radar measurements. Atmos. Res. 59–60, 283–293.

Gosset, M., Zawadzki, I., 2001. Effect of nonuniform beam filling on the propagation of the radar signal at X-band frequencies. Part I: changes in the $k(Z)$ relationship. J. Atmos. Oceanic Technol. 18, 1113–1126.

Illingworth, A.J., Johnson, M.P., 1999. The role of raindrop shape and size spectra in deriving rainfall rates using polarization radar. In: 29th Conference on Radar Meteorology. American Meteorological Society, Montreal, Canada, pp. 301–304.

Joss, J., Gori, E.G., 1978. Shapes of raindrop size distribution. J. Appl. Meteorol. 17, 1054–1061.

Joss, J., Lee, R., 1995. The application of radar-gauge comparisons to operational precipitation profile corrections. J. Appl. Meteorol. 34, 2612–2630.

Joss, J., Waldvogel, A., 1970. A method to improve the accuracy of radar measured amounts of precipitation. In: 14th Conference on Radar Meteorology. American Meteorological Society, Tucson, pp. 237–238.

Joss, J., Zawadzki, I., 1997. Raindrop size distribution again? In: 28th Conference on Radar Meteorology. American Meteorological Society, Austin, TX, pp. 326–327.

Keenan, T.D., Carey, L.D., Zrnic, D.S., May, P.T., 2001. Sensitivity of 5-cm wavelength polarimetric radar variables to raindrop axial ratio and drop size distribution. J. Appl. Meteorol. 40, 526–545.

Koistinen, J., Puhakka, T., 1984. Can we calibrate radar with raingagues? In: 22rd Conference on Radar Meteorology. American Meteorological Society, Zurich, Switzerland, pp. 263–267.

Krajewski, W.F., 1987. Cokring radar-rainfall and rain gage data. J. Geopys. Res. 92 (D8), 9571–9580.

Krajewski, W.F., Ahnert, P.R., 1986. Near real-time tests of multivariate analysis system. In: 23rd Conference on Radar Meteorology and Cloud Physics Conference. American Meteorological Society, Snowmass, CO, pp. JP66–JP69.

Lee, G.W., 2003. Errors in rain measurement by radar: effect of variability of drop size distributions. Ph.D. Thesis, McGill University, 279pp.

Lee, G.W., Zawadzki, I., 2003. Sequential intensity filtering technique (SIFT): filtering out noise to highlight the physical variability of drop size distributions. In: 31st Conference on Radar Meteorology. American Meteorological Society, Seattle, pp. 18—21.

Lee, G.W., Zawadzki, I., Szyrmer, W., Sempere-Torres, D., Uijlenhoet, R., 2004. A general approach to double-moment normalization of drop size distributions. J. Appl. Meteorol. 43, 264—281.

Lee, G., Zawadzki, I., 2005a. Variability of drop size distributions: time scale dependence of the variability and its effects on rain estimation. J. Appl. Meteorol. 44, 241—255.

Lee, G.W., Zawadzki, I., 2005b. Variability of drop size distributions: noise and noise filtering in disdrometric data. J. Appl. Meteorol. 44, 264—281.

Marshall, J.S., Palmer, W.McK., 1948. The distribution of raindrops with size. J. Meteorol. 5, 165—166.

Miriovsky, B.J., Bradley, A.A., Eichinger, W.E., Krajewski, W.F., Kruger, A., Nelson, B.R., Creutin, J.-D., Lapetite, J.-M., Lee, G.W., Zawadzki, I., Ogden, F.L., 2004. An experimental study of small-scale variability of radar reflectivity using disdrometer observations. J. Appl. Meteorol. 43, 106—118.

Mishchenko, M.I., Hovenier, J.W., Travis, L.D., 2000. Light Scattering by Nonspherical Particles. Academic Press, New York, 690pp.

Pruppacher, H.R., Beard, K.V., 1970. A wind tunnel investigation of the internal circulation and shape of water drops falling at terminal velocity in air. Quart. J. Roy. Meteor. Soc. 96, 247—256.

Richard, W.G., Crozier, C.L., 1983. Precipitation measurement with a C-band weather radar in Southern Ontario. Atmos.-Ocean 21, 125—137.

Sheppard, B.E., 1990. Measurement of raindrop size distribution using a small Doppler radar. J. Atmos. Oceanic Technol. 7, 255—268.

Sheppard, B.E., Joe, P.I., 1994. Comparison of raindrop size distribution measurements by a Joss—Waldvogel disdrometer, a PMS 2DG spectrometer, and a POSS Doppler radar. J. Atmos. Oceanic Technol. 11, 874—887.

Smith, P.L., Zhong, L., Joss, J., 1993. A study of sampling-variability effects in raindrop size observations. J. Appl. Meteorol. 32, 1259—1269.

Smyth, T.J., Illingworth, A.J., 1998. Radar estimates of rainfall rates at the ground in bright band and non-bright events. Quart. J. Roy. Meteor. Soc. 124, 2417—2434.

Steiner, M., Smith, J., 2004. Scale dependence of radar-rainfall rates. An assessment based on raindrop spectra. J. Hydrometeorol. 5, 1171—1180.

Wilson, J.W., Brandes, E.A., 1979. Radar measurement of rainfall — a summary. Bull. Am. Meteor. Soc. 60, 1048—1979.

Zawadzki, I.I., 1975. On radar-rain gauge comparison. J. Appl. Meteorol. 6, 1430—1436.

Zawadzki, I., 1984. Factors affecting the precision of radar measurements of rain. In: 22nd Conference on Radar Meteorology. American Meteorological Society, Zurich, pp. 251—256.

Zawadzki, I., Lee, G.W., Bellon, A., 2002. Bias and random errors in radar measurements of precipitation and their scale dependence for QPF validation. In: The World Weather Research Programme's (WWRP) International Conference on Quantitative Precipitation Forecasting, Reading, UK, Royal Meteorological Society, vol. 1, p. 26. Online proceeding is available at: <http://www.royal-met-soc.org.uk/entry/qpfproc.html>.

Zrnic, D.S., Ryzhkov, A.V., 1999. Polarimetry for weather surveillance radars. Bull. Am. Meteor. Soc. 80, 389—406.